Proc. Natl. Acad. Sci. USA
Vol. 78, No. 11, pp. 6981–6985, November 1981
Cell Biology

Rotational diffusion of epidermal growth factor complexed to cell surface receptors reflects rapid microaggregation and endocytosis of occupied receptors

(membrane dynamics/phosphorescence anisotropy/receptor clustering/hormone)

RAPHAEL ZIDOVETZKI*, YOSEF YARDEN†, JOSEPH SCHLESSINGER†‡, AND THOMAS M. JOVIN*‡

*Abteilung Molekulare Biologie, Max Planck Institut für Biophysikalische Chemie, Postfach 968, D-3400 Göttingen, Federal Republic of Germany; and †Department of Chemical Immunology, The Weizmann Institute of Science, Rehovot, Israel

Communicated by Manfred Eigen, August 18, 1981

ABSTRACT **The rotational diffusion of epidermal growth factor (EGF)–receptor complexes on living human epidermoid carcinoma cells (A-431) has been measured by phosphorescence emission and anisotropy in the μs time domain. A biologically active phosphorescent conjugate of EGF, erythrosin-EGF, was applied to living cells. The hormone–receptor complexes were mobile with rotational correlation times in the range 25–90 μs when labeled and measured at 4°C. Prolonged incubation and exposure to higher temperatures (23 and 37°C) resulted in longer times up to 350 μs, indicative of the progressive formation of microclusters, estimated to contain 10–50 receptors. Upon internalization of the hormone–receptor complexes, visible patches were observed by fluorescence microscopy, and the rotational correlation times were shorter, indicating a decrease in size of the dynamic unit. The sign of the rotational relaxation also varied with localization and processing of the hormones. The rate of lateral diffusion of EGF–receptor complexes, measured under similar conditions by fluorescence photobleaching recovery, increased with temperature in contrast to the rotational motion.**

Epidermal growth factor (EGF) is a polypeptide of low molecular mass (6045 daltons) isolated from the submaxillary glands of adult male mice (1). EGF stimulates the proliferation of various fibroblasts, epidermal and epithelial cells *in vitro* and *in vivo* (1). The first step in the action of EGF is binding to a specific membrane receptor on target cells, identified as a 170,000- to 190,000-dalton glycoprotein (2–4). The binding of EGF to the membrane receptors initiates a chain of diverse physiological processes. Prompt responses include enhancement of protein phosphorylation, increased ion and metabolite transport, activation of cytoplasmic enzymes, and changes in cellular morphological characteristics (5) and cytoskeletal organization (6). It has been reported that EGF binds to diffusely distributed membrane receptors (7–10), which rapidly redistribute so as to cluster in a temperature-sensitive process over coated regions of the plasma membrane (10). The latter endocytose and form coated vesicles inside the cell, which later interact with other intracellular organelles. The hormone is finally degraded (1, 10, 11).

Visualization by electron microscopy of ferritin-EGF bound to A-431 human epidermoid carcinoma cells (12), which are unusually rich in EGF receptors (2×10^6 per cell), has revealed the formation of microclusters composed of 5–10 ferritin-EGF molecules within 1–2 min at 37°C (10). It was argued that the formation of microclusters of EGF–receptors is required for the induction of DNA synthesis and for the processing of the membrane-bound EGF molecules (13, 14).

In this report we describe measurements of the rotational diffusion of EGF–receptor complexes on A-431 cells. The EGF receptors on living cells were labeled with a biologically active phosphorescent derivate of EGF, erythrosin-EGF (Er-EGF). Cells in suspension were excited by a laser pulse, and the phosphorescence emission and anisotropy were recorded as a function of time. This method is well suited to the study of rotational motions in membranes in the μs–ms time range (15, 16). The measurements were augmented by lateral diffusion determinations by the method of fluorescence photobleaching recovery (FPR) with fluorescent derivatives of EGF and by biochemical determinations of cellular localization and degradation of the hormone with optical and radioisotope techniques.

Cells labeled with hormone at 4°C typically showed rotational correlation times of 25–50 μs, values we attribute to single or partially aggregated receptors. At higher temperatures (23 and 37°C), the rotational correlation times were characteristically longer and, thus, provided evidence for the microclustering of EGF–receptor complexes. The correlation times and the corresponding amplitudes were found to depend on the degree of internalization and degradation of the hormone–receptor complexes.

MATERIALS AND METHODS

Reagents. EGF was purified from male mouse submaxillary glands as described (17). ^{125}I-Labeled EGF (^{125}I-EGF) was prepared by the chloramine T method (18). EGF labeled at the α amino group with either tetramethylrhodamine isothiocyanate (R-EGF) or with erythrosin isothiocyanate (ref. 19; gift of P. Garland) was prepared as described (20). The binding affinities of either Er-EGF or R-EGF to A-431 cells were similar to that of native EGF. Their potency in stimulating DNA synthesis in human foreskin fibroblasts was 80% of native EGF. 3,3'-Dioctadecylindocarbocyanine iodide was a gift from A. Waggoner. The phosphorescence measurements were done in phosphate-buffered saline: 137 mM NaCl/2.7 mM KCl/7.9 mM Na_2NPO_4/1.5 mM KH_2PO_4/0.87 mM $CaCl_2$/0.5 mM $MgCl_2$, pH 7.2.

Cells and Culture. Human epidermoid carcinoma cells (A-431) (12) provided by G. Todaro were grown in Dulbecco's modified Eagle's medium with 10% (vol/vol) fetal calf serum in 10% CO_2/90% air.

Determinations of Binding and Processing of EGF. Binding studies were performed in multidish trays. Each 15-cm well contained approximately 3×10^5 cells. Before the experiments, the cells were washed with 1 ml of prewarmed phosphate-buffered saline. The binding was performed in 0.4 ml of medium.

The publication costs of this article were defrayed in part by page charge payment. This article must therefore be hereby marked "*advertisement*" in accordance with 18 U. S. C. §1734 solely to indicate this fact.

Abbreviations: EGF, epidermal growth factor; Er-EGF, EGF labeled in the α-amino group with erythrosin; R-EGF, EGF labeled in the α-amino group with tetramethylrhodamine; FPR, fluorescence photobleach recovery; ^{125}I-EGF, ^{125}I-labeled EGF.

‡To whom reprint requests should be addressed.

In some of the experiments ^{125}I-EGF was added to A-431 cells attached to the dishes. In other binding experiments, ^{125}I-EGF was added to cells that were suspended with EDTA (8 mM for 7 min at 37°C). Nonspecific binding was measured in the presence of an excess of unlabeled EGF (usually 6 μg/ml). Unbound radioactivity was removed with 3 ml of ice-cold phosphate-buffered saline. The cells were solubilized with 1 ml of 0.1 M NaOH, and their radioactive content was determined.

The effect of 120 μm chloroquine (1 hr at 37°C) on the degradation of ^{125}I-EGF was determined as described (21). A-431 cells were exposed to ^{125}I-EGF by protocols P3 and P4 (see below) and then treated with 6 M urea/3 M acetic acid/1.5 mM phenylmethylsulfonyl fluoride. After centrifugation, the supernatants were applied to Sephadex G-15 columns and eluted with 0.5 M acetic acid/0.1% bovine serum albumin. Intact EGF appeared as a sharp peak after the void volume, and the degradation products appeared as a second peak after $\approx$ 3 void volumes.

Measurements of Lateral Diffusion. The lateral mobility of the receptors was measured by the FPR method (22, 23). We have added a silicon intensified target camera, which can detect low levels of light and is used for aligning and focusing the laser beam on the cell membrane. The fluorescent preparations were observed with Zeiss microscopes (Universal, or an inverted microscope IM-35). Photographs were taken on Kodak Tri-X.

Measurements of Rotational Diffusion by Time-Resolved Phosphorescence Anisotropy. The basic features of the spectrometer used for time-resolved measurements of polarized phosphorescence have been described (15, 16). Excitation of labeled samples (cell suspension of 1–10 $\times$ 10^6 cells per ml) was at 515 nm. Individual records were generated at a frequency of about 10 Hz and averaged. Thus, m records, each consisting of n successive determinations of the parallel and perpendicular polarized emission components ($I_\parallel$, $I_\perp$) were superimposed (typically m = 64, n = 32). Blank corrections were made by subtracting records generated under identical conditions except for the obstruction of the laser excitation. Data were analyzed by multiexponential nonlinear regression techniques (program written by Leon Avery) in a DEC PDP 11 minicomputer.

Preparation of Cellular Samples for Phosphorescence Measurements. In general, confluent cultures (3 $\times$ 10^6 cells per 9-cm plate) were used for labeling with Er-EGF by the following protocols. (P1) Cells were removed from the plates by 10-min incubation with 8 mM EDTA at 37°C and resuspended in medium or phosphate-buffered saline. Labeling with Er-EGF (200 ng/ml) was at 4°C for 1–5 min. The cells were then washed with cold saline and resuspended. (P2) Cells were treated as in P1, but all procedures were at 37°C. (P3) Cells were labeled with Er-EGF (150 ng/ml) in medium at 37°C for 10 min on the plates. They were then removed with EDTA and resuspended. (P4) Cells were treated as in P3, but the cells were preincubated prior to labeling for 1 hr with 120 μM chloroquine, which was subsequently present through the measurements.

Cell suspensions that were used for phosphorescence measurements were in general purged of dissolved O_2 by introducing a continuous argon flow into the cuvettes and agitating gently with a Teflon plunger.

Analysis of Time-Resolved Phosphorescence Data. The following functions were calculated: $S(t) = I_\parallel + 1.6\, I_\perp$; $r(t) = (I_\parallel - I_\perp)/S(t)$. The factor of 1.6 instead of 2 in the first equation reflects the finite aperture of the emission optics (24). $S(t)$ is a measure of the total phosphorescence emission, and its multiexponential analysis yields the phosphorescence (triplet) lifetimes τ_i. $S(t) = S_0 \Sigma_i \beta_i e^{-t/\tau_i}$; $\Sigma \beta_i = 1$.

The emission anisotropy $r(t)$ is a measure of the rotational relaxation of the phosphorescent probe and the macromolecules to which it is attached. For a rigid body exhibiting rotational and librational (wobbling) motions about a molecular symmetry axis oriented at some angle to the membrane, normal $r(t)$ can be represented as a sum of exponential terms of the form $r(t) \simeq \Sigma_j \alpha_j e^{-t/\phi_j} + r_\infty$; $\Sigma \alpha_j = r_{in} - r_\infty$, where the coefficients α_j are related to the angles made by the emission and absorption transition moments to each other and to the rotation axis, and the time constants ϕ_j (i.e., correlation times) are functions of the rotational diffusion coefficients about the molecular axes and (in the case of wobbling motions) the nature and extent of the excursion cone (25). The constant limiting anisotropy at "infinite" time r_∞ is a function of the angles between the rotation axis and absorption (θ_a) and emission (θ_e) transition moments, as well as the orientational order parameter S. The initial anisotropy r_{in} in the absence of Brownian motion is a function only of the angle δ between the absorption and transition moments:

$$r_{in} = \frac{2}{5} P_2(\cos\delta);\ r_\infty = \frac{2}{5} P_2(\cos\theta_a) P_2(\cos\theta_e) S^2 \qquad [1]$$

where $P_2(x) = (3x^2 - 1)/2$ is the second Legendre polynomial (25). The value of S reflects the degree of the wobbling motions about a molecular symmetry axis. In the limits of isotropic motion or strictly uniaxial rotation, S has the value of 0 and 1, respectively. In general, the experimental value of r_{in} will reflect the combined rotational depolarization due to local probe and segmental protein motions in the time domain faster than that examined experimentally.

In the event that $S(t)$ is multiexponential, the analysis of $r(t)$ is more complicated because the observed value is a time-dependent average of possibly various r_i, each weighed by a corresponding S_i. In our case, we determined that the excited state lifetimes τ_i were essentially the same for the isolated Er-EGF probe and its various complexes with the cell.

RESULTS

The Time-Course of EGF Interaction with Attached and Suspension Cells Differs. The apparatus used for the measure-

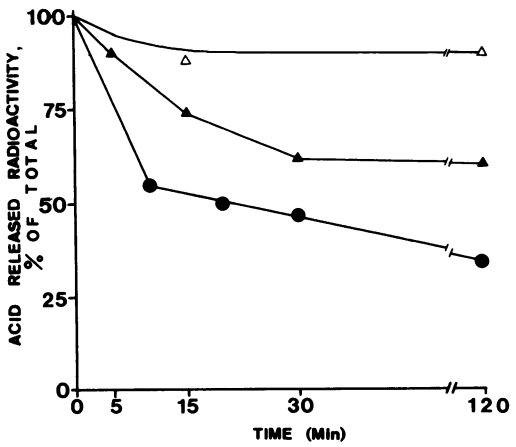

FIG. 1. Time course of ^{125}I-EGF internalization. (*i*) Cells in suspension. Monolayers of A-431 cells were harvested with 8 mM EDTA in Tris/saline buffer, centrifuged, and resuspended in phosphate-buffered saline (5 $\times$ 10^5 cells per 100-μl aliquot in a conical tube), and then were incubated for the indicated times with ^{125}I-EGF (10 ng/ml) at either 4°C (△) or 37°C (▲). (*ii*) A-431 cells were grown to confluency in 24-well Costar trays. Before use, the monolayers were washed with 1 ml of phosphate-buffered saline, and 0.4 ml of 0.1% bovine serum albumin containing ^{125}I-EGF (10 ng/ml) was added and incubated at 37°C (●). At the indicated times, the cells were washed extensively with ice-cold saline and treated with 0.2 M acetic acid/0.5 M NaCl, pH 2.5, for 6 min at 4°C. The acid-extracted radioactivity and that remaining in association with the cells were counted and corrected for nonspecific binding.

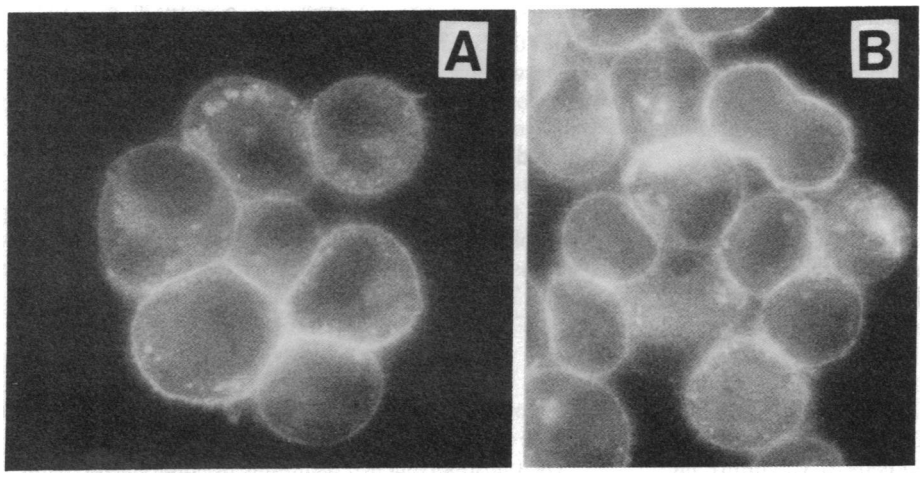

FIG. 2. The distribution of R-EGF (50 ng/ml) on A-431 cells in suspension labeled for 15 min at 37°C, washed with phosphate-buffered saline, then allowed to settle on glass coverslips. (*A*) Cells observed after 15 min at 37°C. (*B*) cells observed after 1 hr at 37°C. (×732.)

ments of phosphorescence requires a suspension of labeled cells. Previous studies of EGF interaction with the A-431 carcinoma line have been limited to attached cells. The contrast in the behavior of cells exposed to ^{125}I-EGF in the attached state as compared to the suspended state was striking (Fig. 1). Thus, cells in suspension were labeled to the same extent, but internalization of the hormone was much slower and degradation was almost undetectable. Fluorescence microscopy of suspended cells labeled with R-EGF revealed that the distribution of the hormone was predominantly diffuse (Fig. 2), with only occasional visible patches that were otherwise present at high density upon prolonged incubations with attached cells (26).

Demonstration by Phosphorescence of EGF Binding to Cells. The phosphorescent properties of the derivative of EGF, Er-EGF, in free solution were those expected for a small polypeptide undergoing free rotation (Fig. 3). As in the case of many protein conjugates of the halogenated fluorescein family of compounds (15), the decay of phosphorescence intensity was multiexponential, with typical time constants of 7, 55, and 150 μs. Er-EGF bound to cellular receptors behaved similarly. The emission was depolarized ($r \approx 0$) in agreement with an expected rotational correlation time of ≈4 ns for this molecule in aqueous media (15). The phosphorescence properties of the Er-EGF attached to its cellular receptors are summarized in Fig. 4. The characteristic feature is a finite emission anisotropy with r_{in} and $r_\infty > 0$. Thus, *the hormone–receptor complex is a relatively rigid structure*. Under all conditions, the anisotropy was time dependent and analyzable in terms of correlation times in the range of 20–350 μs. However, the fact that r_∞ never approached 0 and, in fact, usually exceeded the initial value r_{in} indicates that rotation of the hormone–receptor complex is hindered.

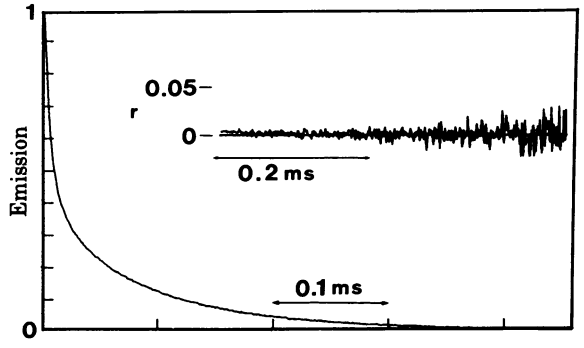

FIG. 3. Phosphorescence intensity decay of Er-EGF in phosphate-buffered saline. The phosphorescence lifetimes are 7, 55, and 150 μs. The corresponding normalized amplitudes are: 0.45, 0.35, and 0.20. (*Inset*) The corresponding anisotropy *r*.

The Rotation of the Er-EGF-Receptor Complex Provides Evidence for Microaggregation. Characteristic rotational correlation times on the order of 25–50 μs were observed after labeling and examination of the cells at 4°C (Table 1). We believe that these values represent the superposed rotational relaxation of single hormone–receptor complexes and of small microclusters (2–3 receptors).

Prolonged incubation (1 hr, 4°C) or elevated temperatures

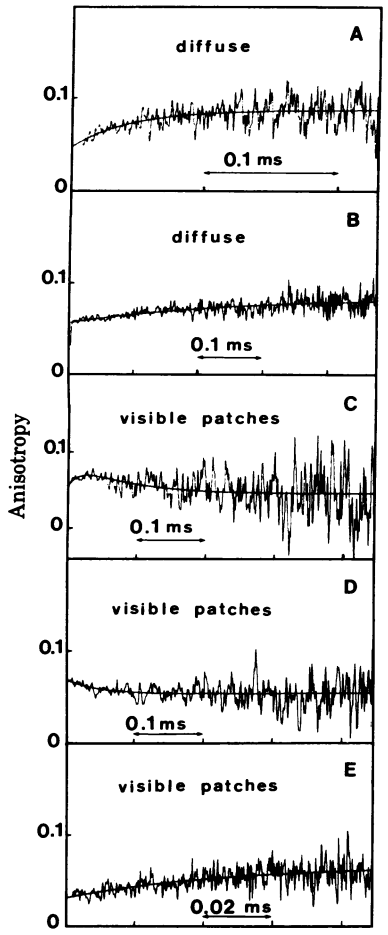

FIG. 4. Anisotropy decay kinetics of Er-EGF–receptor complexes. The smooth lines represent the results of the computer analysis (Table 1). (*A*) Condition P1, short incubation. (*B*) Condition P2. (*C*) Condition P3, 20 min incubation. (*D*) Condition P3, incubation for 1.5–4 hr. (*E*) Condition P4, incubation for 1.5–4 hr. The distribution of R-EGF under corresponding conditions as visualized by fluorescence microscopy is given for each case.

(23 and 37°C in suspension) led to a lengthening of the rotational correlation times (Fig. 4; Table 1). Thus, at 37°C, values up to 350 μs were observed. Under these conditions, the distribution of bound Er-EGF was still diffuse by microscopy. The molecular species undergoing rotation are thus of a size below the resolution of the light microscope.

The amplitude of the rotational relaxation of Er-EGF bound to the cell surface was negative ($\alpha < 0$; Table 1). This finding suggests that the orientation of the probe to the molecular rotation axis is not random. Furthermore, the probe is relatively inaccessible to the external medium because the quenching of phosphorescence emission by O_2 (air-equilibrated medium) shortened the lifetime of bound Er-EGF only by factor of 3, whereas it fully quenched the emission of Er-EGF in solution.

The Rotational Behavior of EGF–Receptor Complexes Changes upon Internalization and Processing. Under conditions favoring internalization (attached cells 37°C: culture medium) the rotational relaxation of the hormone–receptor complex changed qualitatively and quantitatively. Upon short incubation times with labeled hormone (≈10 min), a biphasic rotational relaxation was observed with a ϕ_{fast} of 20 μs (negative amplitude) and a ϕ_{slow} of 60 μs (positive amplitude). The faster component disappeared upon prolonged incubation (Fig. 4; Table 1). The relaxation process with positive amplitude was not observed upon incubation in the presence of chloroquine (Fig. 4; Table 1), an agent that suppresses lysosomal degradation (27).

Quantitative analysis by gel filtration chromatography and the evaluation of the degree of accessibility to acetic acid (i.e., surface localization) of the cell-associated ^{125}I-EGF showed that, in the presence of chloroquine, more than 90% of the EGF originally bound to the cells remained bound after 2 hr at 37°C, and much less (50%) remained bound in the absence of chloroquine. Under both conditions, only 2% of the cell-associated EGF was degraded. This implies that degradation products are rapidly released into the medium.

The Lateral Diffusion of EGF Receptors and a Lipid Probe on A-431 Cells. The lateral diffusion of R-EGF and of the lipid probe 3,3′ dioctadecylindocarbocyanine iodide bound to A-431 cells was measured with the FPR apparatus combined with a video intensification visualization system. This allows the correlation between receptor localization and mobility on living cells.

A-431 cells were labeled for 30 min at 4°C with R-EGF (50 ng/ml), and the lateral diffusion of the occupied receptors was measured at various temperatures. The lateral diffusion coefficients D_t at 4, 23, and 37°C were 3×10^{-10}, 6×10^{-10}, and 8.5×10^{-10} cm^{2}sec^{-1}, respectively. The fraction of mobile molecules was 90% at 4°C and 45% after 10 min at 37°C. Under the latter conditions, patches and endocytic vesicles containing R-EGF were seen, but part of the R-EGF remained diffusely distributed on the surface of the A-431 cells. The decrease in %R reflects the immobility of the visible patches on the experimental time scale. A full analysis of the temperature dependence of the lateral mobility of EGF receptors and its possible relationship to the formation of patches will be published elsewhere. The lateral diffusion coefficient of the lipid probe was 2×10^{-8} cm^{2}sec^{-1} at 23°C on these cells.

Table 1. Summary of the phosphorescence anisotropy decay parameters for different states of Er-EGF complexes with A-431 cells

Labeling conditions					
°C	Plate* or suspension†	Incubation, min	r_∞	ϕ, μs	α
4	Both	≈5	0.08	25–50	−0.040
4	Suspension	>60	0.07	95	−0.033
23	Suspension	>5	0.08	140	−0.023
37	Suspension	>5	0.08	200–350	−0.026
37	Plate	20	0.04	20‡	−0.046‡
				60§	0.046§
37	Plate	>90	0.05	50	0.018
	Plate + chloroquine	>90	0.05	26	−0.025

We estimate the error for most parameters as ±20%. The range is given in cases where larger variations were obtained, probably due to slight differences in biological response (e.g., receptor clustering).
* In medium.
† In phosphate-buffered saline.
‡ Fast component (see Fig. 4*C*).
§ Slow component (see Fig. 4*C*).

DISCUSSION

This work shows that the rotational motions of cell surface receptors for hormones can be measured on living cells.

The phosphorescence technique has high sensitivity in terms of concentration requirements (equivalent to about 1 nM chromophore) and temporal resolution (0.3 μs to 1 ms). The results are consistent with and complementary to those obtained with very different biochemical and fluorescent techniques.

We have observed a clear progression of physical states of the EGF-receptor complexes which must bear a relationship to the mechanisms eliciting the various biological responses. The hormone–receptor complexes located on the cell surface demonstrate a characteristic pattern of rotational relaxation with correlation times ranging from 25 to 350 μs. We will attempt a molecular interpretation of these values using the simplest model, that of uniaxial rotation of a rigid integral membrane protein (28). A biexponential decay is predicted for this mode of rotation with two time constants ϕ and $\phi/4$ where $\phi = 4V\eta/kT$ (28). V is the volume of the presumed cylindrical protein, η is the viscosity of its immediate environment, k is Boltzmann's constant, and T is the absolute temperature. Unfortunately, the fraction of the entire receptor molecule (150,000–170,000 daltons) that is embedded in the membrane [and thus determines the rotational dynamics (29)] is unknown. An upper estimate for ϕ is obtained by assuming a V that uses the entire mass of the receptor, a value of 0.72 for the partial specific volume, and a membrane apparent viscosity of about 1 and 4 P at 37°C and 4°C, respectively (30). The corresponding values of ϕ are 20 μs at 37°C and 92 μs at 4°C, and they compare favorably with the measurements at 4°C (Table 1). The fact that the data are adequately described by a single rotation correlation time and not the two expected for uniaxial rotation probably derives from the level of irreducible noise, the inapplicability of the representation of the hormone–receptor complex as a strictly rigid entity, and nonequivalent amplitudes for the two components (16). We conclude tentatively that at 4°C, the observed values correspond to a weighted average representing motions of independent receptors and of clusters of limited size.

The dramatic finding is that the rotation becomes *slower* as the temperature increases, although the increase in membrane fluidity should produce the opposite effect. The simplest interpretation is that the size of the rotating entity is increasing. The existence of receptor microclusters induced by hormone binding and their possible significance in the pathways leading to the pleiotropic biological responses have been extensively discussed (13, 14). The rotational diffusion measurements presented here provide physical evidence for these entities in the living cell. The rotational correlation times of ≈200–350 μs at 37°C could correspond to a maximum cluster size of 40–50 receptors if the aggregates are more extended. The lateral interactions stabilizing the clusters must be strong in order to confer the degree of rigidity observed for the total structure. However, the size of the microclusters is self-limited because complete immobilization is not observed.

The hormone–receptor complex on the cell surface has other interesting properties. The hormone binding site appears to be deeply embedded in the cell membrane as judged by its inaccessibility to O_2. Furthermore, the chromophore exhibits a rather fixed orientation to the rotation axis, as judged from the negative rotational relaxation amplitudes (Table 1). From equation 1 it can be inferred that both transition moments are located in the range $0° < \theta_a, \theta_e < 54°$ relative to the rotation axis and are more or less coplanar with it. This behavior has been observed with numerous other membrane components tagged with halogenated fluorescein probes (ref. 15; unpublished data) and may reflect a preferred disposition of these molecules to the plane of the membrane.

Prolonged incubation of the attached cells in the presence of chloroquine, a drug that inhibits degradation but not internalization of the hormone–receptor complex, led to a reduction in the rotational correlation time. Thus, it appears that microclusters decrease in size with perhaps less than 5–10 receptors typically in association. These findings correspond to conditions under which visible patches are observed by fluorescence microscopy, implying that in these larger entities originating from coated vesicles and identified as multivesicular bodies (10), *the receptors are distributed in relatively small dynamically independent domains.* Under conditions favoring internalization the rotational relaxation amplitudes inverted in sign (Fig. 4*D*). The controls with ^{125}I-EGF showed that most of the degraded hormone was released by the cells to the outer medium and, thus, was not detected in the phosphorescence measurements. The implication is that the hormone or associated receptor, or both, assumed a different orientation in the membrane, possibly during the incipient steps of degradation. The negative component seen after short incubation at 37°C (Fig. 4*C*) and in the presence of chloroquine suggests that the drug blocks processing at some stage in the transfer from coated vesicles through multivesicular bodies to lysosomes (26). An unambiguous interpretation of the results obtained upon conditions of internalization is difficult due to the superposition of many states.

Changes in the values of r_{in} and r_∞ provide information about the limiting states of the hormone–receptor complex. Thus, the relatively low values of r_{in} are indicative of some limited rapid motion exhibited by the chromophore at its attachment site or by segmental excursions of the polypeptide, or both. r_∞ varies considerably according to the location of the hormone. From Eq. 1, either changes in probe orientation (θ_a, θ_e) or in orientational order parameter (S), or both, are responsible. The high values of r_∞ exhibited by the cell surface complexes (Table 1) imply that the orientational order is very high (i.e., the motions normal to the molecular symmetry axis are minimal and S is not appreciably less than 1).

It is notable that the lateral diffusion coefficient of the lipid probe, $D_L = 2 \times 10^{-8}$ cm^{2}sec^{-1} at 23°C, is much higher than that of the receptor, $D_P = 6 \times 10^{-10}$ cm^{2}sec^{-1} at the same temperature. The following expression for the translational diffusion coefficient was suggested for cylindrical molecules in membranes (29):

$$D_t = \frac{kT}{4\pi\eta h} \times \left(\ln\frac{h\eta}{a\eta_1} - 0.507\right)$$

where h is the thickness of the membrane, a is the radius of the molecule, and η_1 is the viscosity of the external medium. The weak dependence of D_t on molecular size given by this formula is incompatible with the difference between D_P and D_L, even assuming the microaggregation of the receptor.

An alternative, free-volume diffusion model gives the following relation betwen D_L and D_P (31): $D_L/D_P = \sqrt{M_P/M_L}$, where M_P and M_L are the molecular weights of the protein and the lipid, respectively. The expression incorporates a stronger dependence on molecular size than that of the Saffman model and is consistent with the experimental ratio of D_L/D_P, assuming microclusters of about five receptors at 23°C. In any event, the rate of lateral diffusion of the receptor increases with temperature, in accordance with the expected influence of membrane fluidity. However, it remains to be established whether interactions with other membrane or cytoplasmic elements (e.g., the cytoskeleton) play a significant role in determining the dynamic properties of the receptor.

This study was supported by a grant from the National Institutes of Health (CA-25820 to J.S.) and from U.S.–Israel Binational Science Foundation (to J.S.). R.Z. is recipient of a Minerva postdoctoral fellowship; Y.Y. is recipient of a short-term European Molecular Biology Organization fellowship.

1. Carpenter, G. & Cohen, S. (1979) *Annu. Rev. Biochem.* **48**, 193–216.
2. Hock, R. A., Nero, E. & Hollenberg, M. D. (1979) *Nature (London)* **277**, 403–405.
3. Wrann, M. M. & Fox, C. F. (1979) *J. Biol. Chem.* **254**, 8083–8086.
4. Cohen, S., Carpenter, G. & King, L., Sr. (1980) *J. Biol. Chem.* **255**, 4834–4842.
5. Chinkers, M., McKanna, J. A. & Cohen, S. (1979) *J. Cell Biol.* **83**, 260–265.
6. Schlessinger, J. & Geiger, B. (1981) *Exp. Cell Res.*, in press.
7. Schlessinger, J., Schechter, Y., Willingham, M. C. & Pastan, I. (1978) *Proc. Natl. Acad. Sci. USA* **75**, 2659–2663.
8. Haigler, H. T., Ash, J. F., Singer, S. J. & Cohen, S. (1978) *Proc. Natl. Acad. Sci. USA* **75**, 3317–3321.
9. Schlessinger, J., Schechter, Y., Cuatrecasas, P., Willingham, M. C. & Pastan, I. (1978) *Proc. Natl. Acad. Sci. USA* **75**, 5353–5357.
10. Haigler, H. T., McKanna, J. A. & Cohen, S. (1979) *J. Cell Biol.* **81**, 382–395.
11. Gorden, P., Carpentier, J. L., Cohen, S. & Orci, L. (1978) *Proc. Natl. Acad. Sci. USA* **75**, 5025–5029.
12. Fabricant, R. N., De Larco, J. E. & Todaro, G. J. (1977) *Proc. Natl. Acad. Sci. USA* **74**, 565–569.
13. Schechter, Y., Hernaez, L., Schlessinger, J. & Cuatrecasas, P. (1979) *Nature (London)* **278**, 835–838.
14. Schlessinger, J. (1980) *Trends Biochem. Sci.* **5**, 210–214.
15. Austin, R. H., Chan, S. S. & Jovin, T. M. (1979) *Proc. Natl. Acad. Sci. USA* **76**, 5650–5654.
16. Jovin, T. M., Bartholdi, M. & Vaz, W. L. C. (1981) *Ann. N. Y. Acad. Sci.* **366**, 176–196.
17. Savage, C. R. & Cohen, S. (1972) *J. Biol. Chem.* **247**, 7609–7611.
18. Hunter, M. W. & Greenwood, F. C. (1962) *Nature (London)* **194**, 495–496.
19. Moore, C. H. & Garland, P. B. (1979) *Biochem. Soc. Trans.* **7**, 945–946.
20. Schechter, Y., Schlessinger, J., Jacobs, S., Chang, K. J. & Cuatrecasas, P. (1978) *Proc. Natl. Acad. Sci. USA* **75**, 2135–2139.
21. Sonne, O. & Gliemann, J. (1980) *J. Biol. Chem.* **255**, 7449–7454.
22. Schlessinger, J., Koppel, D. E., Axelrod, D., Jacobson, K., Webb, W. W. & Elson, E. L. (1976) *Proc. Natl. Acad. Sci. USA* **73**, 2409–2413.
23. Axelrod, D., Koppel, D. E., Schlessinger, J., Elson, E. L. & Webb, W. W. (1976) *Biophys. J.* **16**, 1055–1069.
24. Jovin, T. M. (1979) in *Flow Cytometry and Sorting*, eds. Melamed, M., Mullaney, P. & Mendelson, M. (Wiley, New York), pp. 137–165.
25. Lipari, G. & Szabo, A. (1980) *Biophys. J.* **30**, 489–506.
26. Yarden, Y., Gabbay, M. & Schlessinger, J. (1981) *Biochem. Biophys. Acta* **674**, 188–203.
27. King, A. C., Hernaez-Davis, L. & Cuatrecasas, P. (1980) *Proc. Natl. Acad. Sci. USA* **77**, 3283–3287.
28. Cherry, R. J. (1978) *Methods Enzymol.* **54**, 47–61.
29. Saffman, P. G. (1976) *J. Fluid Mech.* **73**, 593–602.
30. Shinitzky, M. & Inbar, M. (1974) *J. Mol. Biol.* **85**, 603–615.
31. Träuble, H. & Sackman, E. (1972) *J. Am. Chem. Soc.* **94**, 4499–4510.